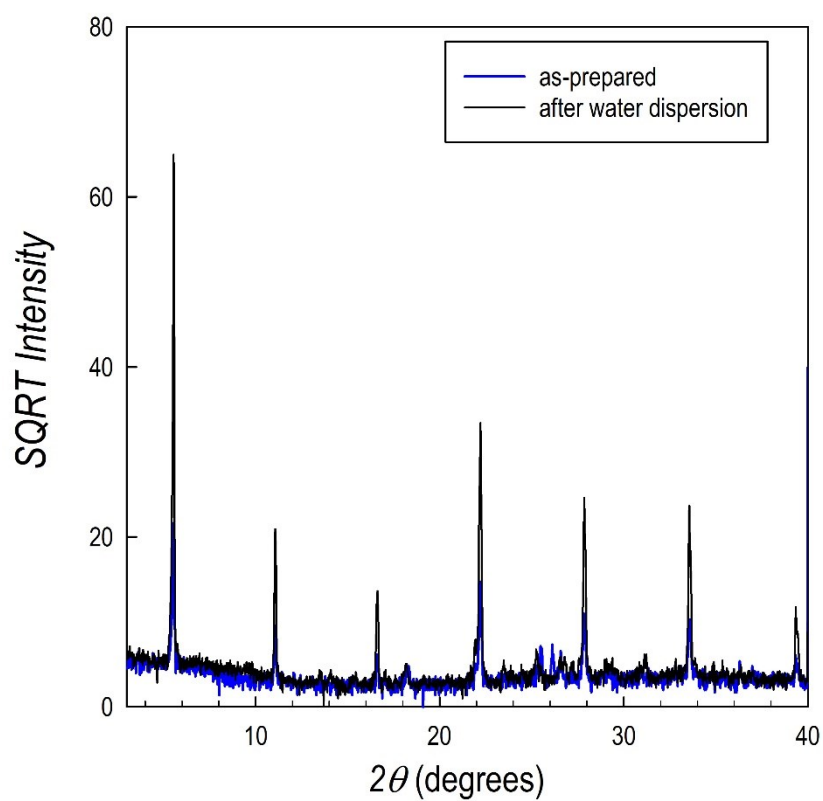
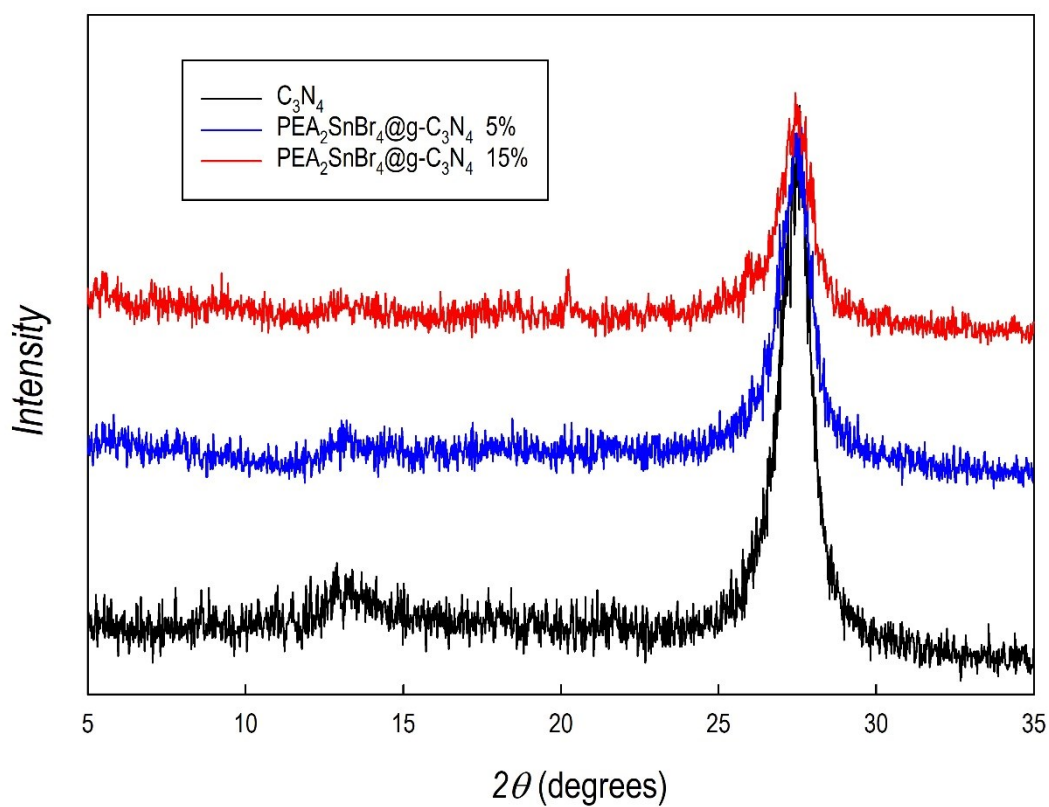


# ELECTRONIC SUPPLEMENTARY INFORMATION



**Figure S1.** XRD (sqrt of intensity) patterns of  $\text{PEA}_2\text{SnBr}_4$  synthesized by wet-chemistry (blue) and after recovery from DW (black)



**Figure S2** – XRD patterns of pure g-C<sub>3</sub>N<sub>4</sub> and PEA<sub>2</sub>SnBr<sub>4</sub>@g-C<sub>3</sub>N<sub>4</sub> composites at different percentages of perovskite loading.

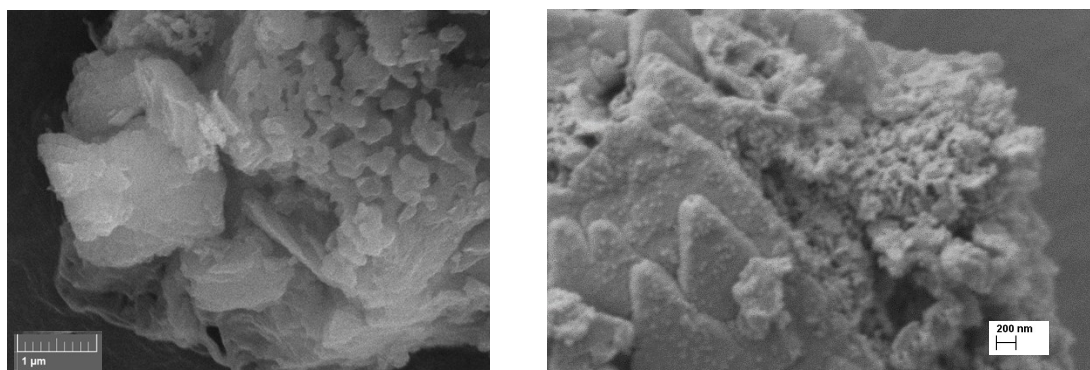


**Figure S3.** Representative SEM images collected on the pristine g-C<sub>3</sub>N<sub>4</sub> (left) and on the PEA<sub>2</sub>SnBr<sub>4</sub>@g-C<sub>3</sub>N<sub>4</sub> composites (15%, right).

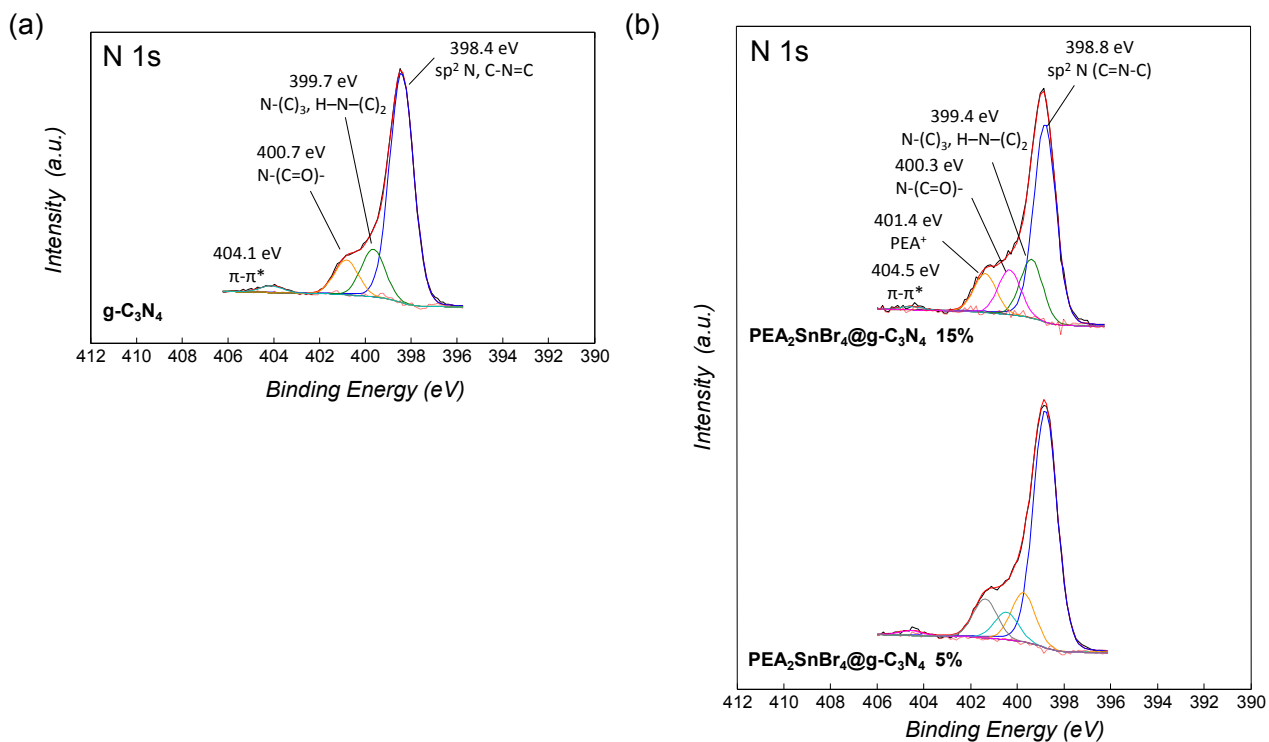


**Figure S4:** XPS N 1s spectra of the pristine  $g-C_3N_4$  (a) and of the  $PEA_2SnBr_4@g-C_3N_4$  composites (b).

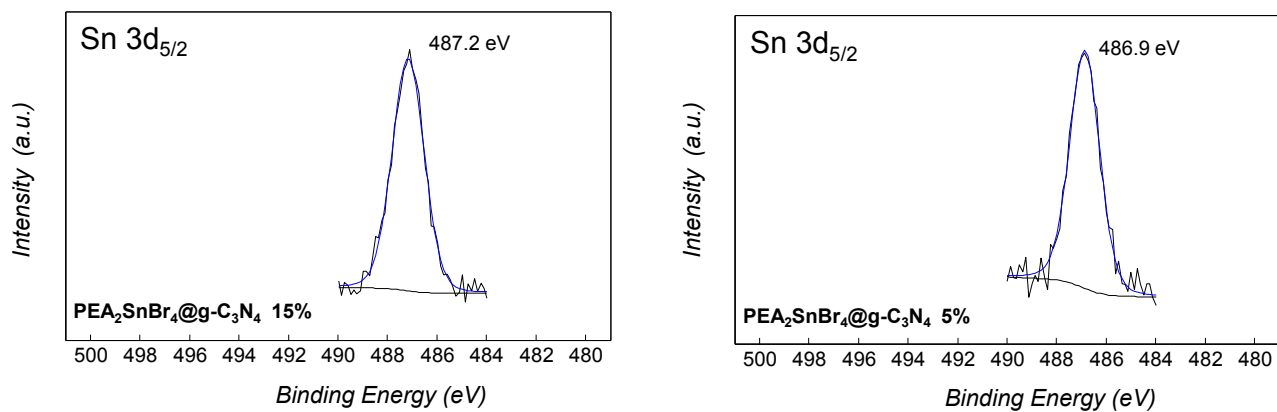


**Figure S5:** XPS Sn 3d<sub>5/2</sub> spectra of the PEA<sub>2</sub>SnBr<sub>4</sub>@g-C<sub>3</sub>N<sub>4</sub> composites.

**Table S1** – Elemental composition of composite samples probed by EDX, e.s.d. for the measurements is around 5%.

Composite (perovskite %)	exp Br/Sn
5	3.79
5	4.04
5	3.91
15	4.02
15	4.01
15	3.96

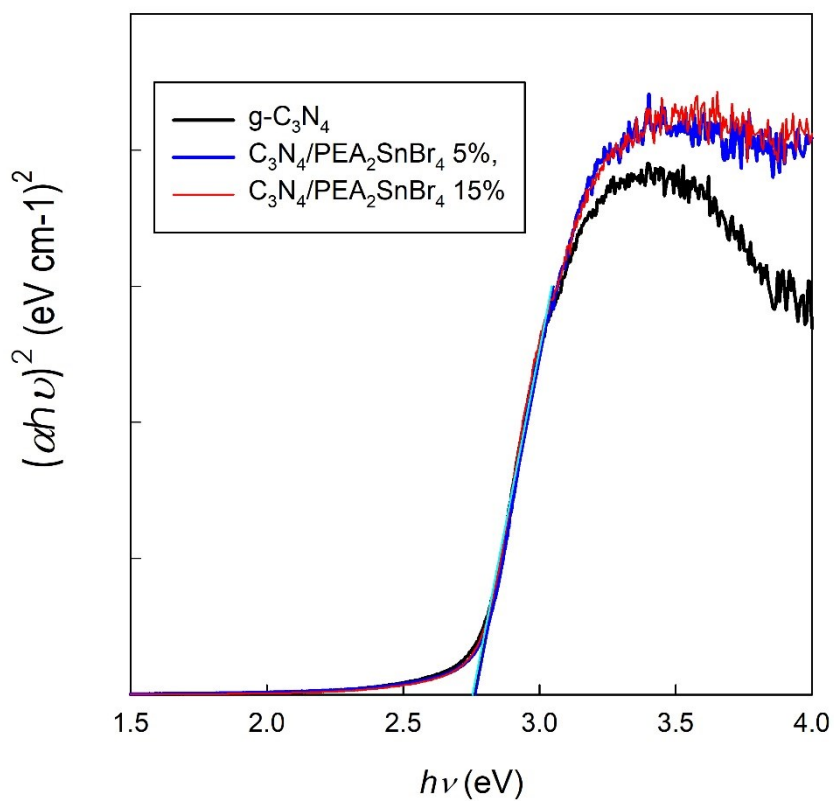


**Figure S6** – Tauc's plots of pure  $g\text{-C}_3\text{N}_4$  and  $\text{PEA}_2\text{SnBr}_4@g\text{-C}_3\text{N}_4$  composites at different percentages of perovskite loading.

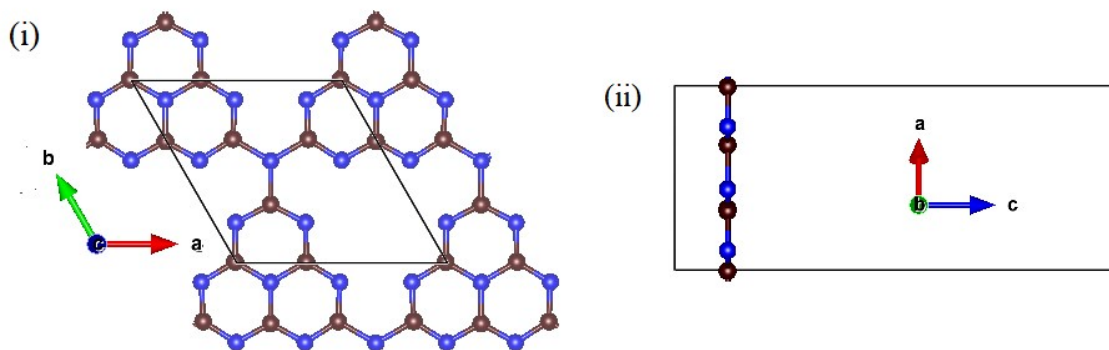


**Figure S7:** Optimized structure of g-C<sub>3</sub>N<sub>4</sub> with highlighted unit-cell in (i) (110), and (ii) (101) planes. The black and blue balls represent C and N atoms, respectively. The unit cell is shown with (i) rhombus and (ii) rectangle.

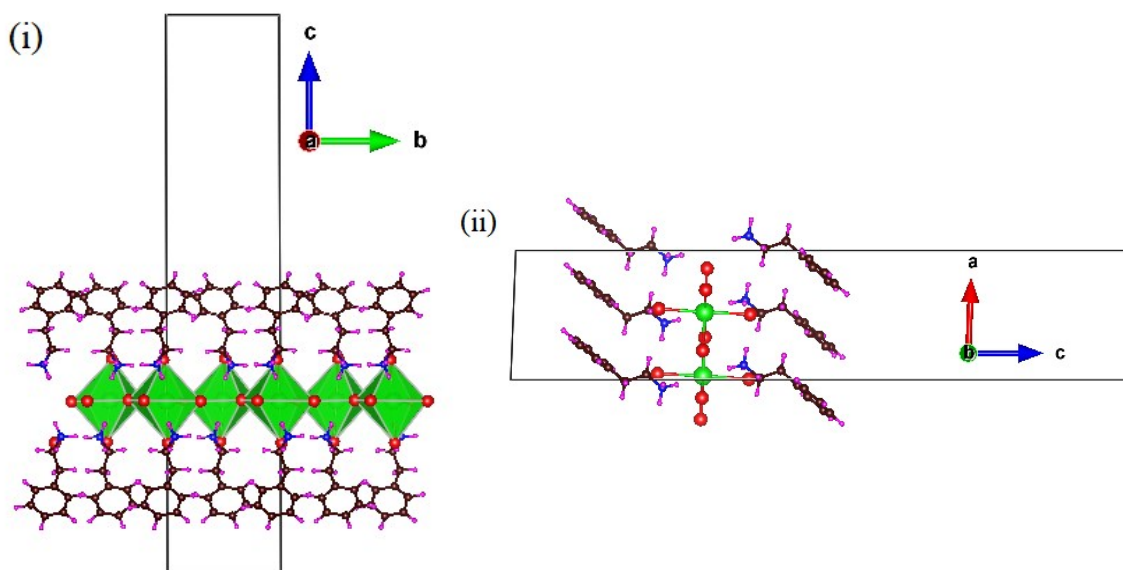


**Figure S8:** Optimized structure of PEA<sub>2</sub>SnBr<sub>4</sub> monolayer in (i) (011) plane, and (ii) (101) plane. The rectangle represent the unit cell. The green, red, black, blue and magenta balls are representative of Sn, Br, C, N, and H atoms, respectively.

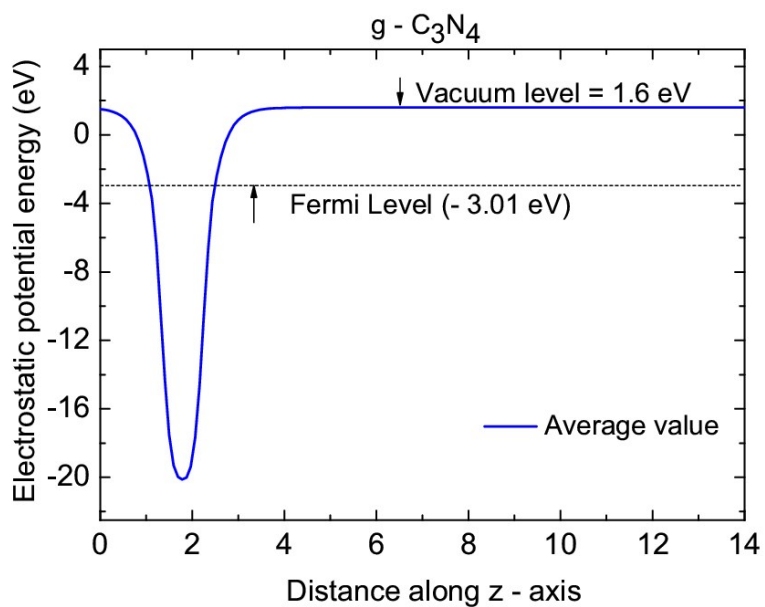


**Figure S9:** Electrostatic potential energy for g-C<sub>3</sub>N<sub>4</sub> plotted along z-axis (Å) of unit cell.

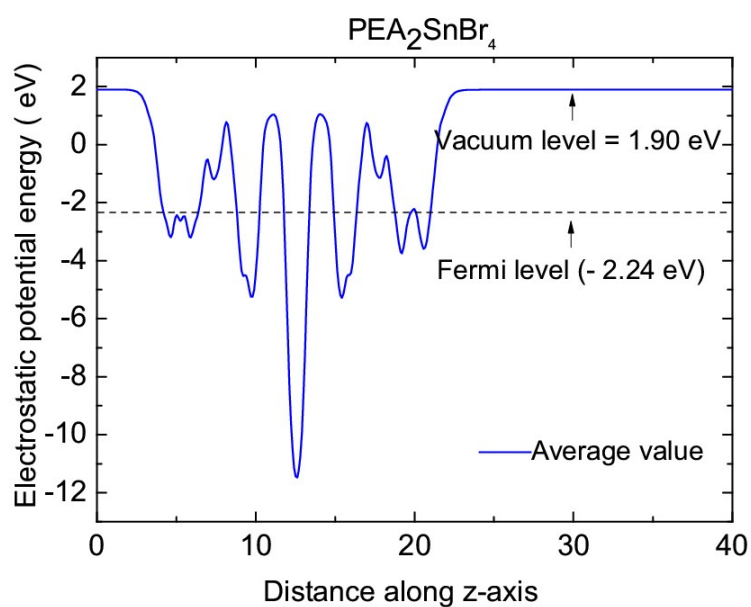


**Figure S10:** Electrostatic potential energy for PEA<sub>2</sub>SnBr<sub>4</sub> monolayer along z-axis (Å).

## Experimental Section

### *Synthesis and characterization of the catalysts*

Bulk g-C<sub>3</sub>N<sub>4</sub> has been synthesized from the polymerization of DCD (NH<sub>2</sub>C(=NH)NHCN, Aldrich, 99%) by the following thermal treatment (under N<sub>2</sub> flux): heating (1°C/min) to 600 °C, isothermal step for 4 hours followed by cooling to room temperature (10°C/min). Synthesis has been carried out in a partially closed alumina crucible. PEA<sub>2</sub>SnBr<sub>4</sub> has been prepared by dissolving PEABr and SnBr<sub>2</sub> in DMF and stirring, under nitrogen flux, the solution until dryness. The PEA<sub>2</sub>SnBr<sub>4</sub>@g-C<sub>3</sub>N<sub>4</sub> composites have been prepared by adding to the DMF solution containing PEABr and SnBr<sub>2</sub> the proper amount of g-C<sub>3</sub>N<sub>4</sub> prepared as described above.

The crystal structure of the samples has been characterized by room temperature Cu-radiation XRD acquired with a Bruker D8 diffractometer. DRS spectra were acquired in the wavelength range 300-800 nm directly on the powders by using a Jasco V-750 spectrophotometer, equipped with an integrating sphere (Jasco ISV-922). Microstructural characterization of the samples was made using a high-resolution scanning electron microscope (SEM, TESCAN Mira 3) operated at 25 kV.

### *H<sub>2</sub> photogeneration and organic dye degradation in water*

H<sub>2</sub> evolution experiments were conducted in distilled water containing 10% v/v triethanolamine (Aldrich, ≥ 99%) or 0.1 M glucose (99.9%, Carlo Erba Reagents), irradiated in Pyrex glass containers (28 mL capacity, 21 mL sample).<sup>1</sup> After addition of the catalyst (1 g L<sup>-1</sup>), the sample was deoxygenated by Ar bubbling (20 min) to obtain anoxic conditions, and irradiated under magnetic stirring for 6 hours.

For the experiments involving use of Pt co-catalyst, Chloroplatinic acid (H<sub>2</sub>PtCl<sub>6</sub>, 38% Pt basis), used as Pt source, was from Sigma-Aldrich. Since Pt is *in situ* photodeposited on the catalyst surface, after Ar bubbling a small volume from a 15 g/L H<sub>2</sub>PtCl<sub>6</sub> aqueous solution was added using a 10-100 μL micropipette to the catalyst suspension (1 g/L) in 10% v/v TEOA or 0.1 M glucose, directly in the photoreactor. The latter was closed with sleeve stopper septa and was irradiated, as described in the following, achieving simultaneous Pt deposition and H<sub>2</sub> production.<sup>2</sup> Irradiation was performed under simulated solar light using a Solar Box 1500e (CO.FO.ME.GRA S.r.l., Milan, Italy) set at a power factor 500 W m<sup>-2</sup>, and equipped with UV outdoor filter made of IR-treated soda lime glass. Duplicate photoproduction experiments were performed on all samples. The headspace evolved gas was quantified by gas chromatography coupled with thermal conductivity detection (GC-TCD), as described in previous work.<sup>1</sup> The results obtained in terms of H<sub>2</sub> evolution rate are expressed in the



paper as  $\mu\text{moles}$  of gas per gram of catalyst per hour ( $\mu\text{moles g}^{-1} \text{h}^{-1}$ ). XRD measurements on spent catalysts have been done by filtering the suspension and recovering the powder, which underwent diffraction measurements.

Methylene blue (MB) degradation tests were performed on  $10^{-5}$  M MB aqueous solutions (150 mL, prepared in distilled water) in presence of 1 g/L of each catalyst, and with no catalyst to evaluate direct photolysis. Before irradiation, magnetic stirring for 30 min in the dark was performed to allow MB adsorption equilibrium on the catalyst. Irradiation was done under simulated solar light ( $250 \text{ W/m}^2$ ): at specific time intervals, 1.5 mL of sample was withdrawn, centrifuged at 3000 rpm for 5 min and the absorbance (664 nm) of the supernatant solution was recorded by an UVmini-1240 UV-vis spectrophotometer (Shimadzu Corporation).

### ***Metal leaching tests***

The leaching tests were performed by dispersion of the as-prepared  $\text{PEA}_2\text{SnBr}_4$  powder in distilled water, under magnetic stirring for 4 h. Then the suspension was filtered on 0.2  $\mu\text{m}$  nylon membrane and the amount of tin in solution was determined by ICP-OES analysis, after acidification (1% v/v ultrapure nitric acid).

### ***XPS Measurements***

XPS analyses were carried out with a Scanning XPS Microprobe (PHI 5000 Versa Probe II, Physical Electronics) equipped with a monochromatic Al  $K_\alpha$  X-ray source (1486.6 eV), operated at 15 kV and 24.8 W, with a spot size of 100  $\mu\text{m}$ . Survey (0–1200 eV) and high resolution spectra (C 1s, O 1s, N 1s, Br 3d and Sn 3d) were recorded in FAT (Fixed Analyser Transmission) mode at a pass energy of 117.40 and 29.35 eV, respectively. Surface charging was compensated using a dual beam charge neutralization system, with a flux of low energy electrons ( $\sim 1$  eV) combined with very low energy positive  $\text{Ar}^+$  ions (10 eV). The hydrocarbon component of C1s spectrum was used as internal standard for charging correction and it was fixed at 284.8 eV. All spectra were collected at an angle of  $45^\circ$  with respect to the sample surface. Best-fitting of the high resolution spectra was carried out with MultiPak data processing software (Physical Electronics).

### ***Computational Details***

The calculations are performed using plane wave projector augmented wave (PAW)<sup>3</sup> pseudopotential method as implemented in Vienna *Ab initio* Simulation Package (VASP).<sup>4</sup> The exchange-correlation functional is treated within generalized gradient approximation (GGA) of Perdew, Burke, and

Ernzerhof (PBE)<sup>5</sup> for structural optimization using  $5 \times 5 \times 1$   $k$ -points mesh. The unit cell dimensions (shape and cell volume) as well as the ionic positions are relaxed until the absolute value of force on each ion becomes less than  $0.005 \text{ eV/\AA}$ . The vacuum spacing between the layers are taken to be  $20 \text{ \AA}$  to eliminate the inter-layer interactions. The optimized structure of g-C<sub>3</sub>N<sub>4</sub> and PEA<sub>2</sub>SnBr<sub>4</sub> monolayers are shown in Figures S4 and S5, respectively. After that, the electrostatic potential energy and band gap values are calculated with Heyd-Scuseria-Ernzerhof (HSE06) hybrid functional.<sup>6</sup> The value of work function is calculated by taking the difference between the Fermi level and the electrostatic potential energy in vacuum (Figures S6 and S7).

## References

- [1] A. Speltini, M. Sturini, D. Dondi, E. Annovazzi, F. Maraschi, V. Caratto, A. Profumo, A. Buttafava, *A. Photochem. Photobiol. Sci.*, **2014**, *13*, 1410-1419.
- [2] L. Yang, J. Huang, L. Shi, L. Cao, Q. Yu, Y. Jie, J. Fei, H. Ouyang, J. A. Ye, *Appl. Catal. B*, **2017**, *204*, 335.
- [3] P. E. Blöchl, *Phys. Rev. B: Condens. Matter Mater. Phys.* **1994**, *50*, 17953-17979.
- [4] G. Kresse, J. Furthmüller, *Phys. Rev. B: Condens. Matter Mater. Phys.* **1996**, *54*, 11169-11186.
- [5] J. P. Perdew, K. Burke, M. Ernzerhof, *Phys. Rev. Lett.* **1996**, *77*, 3865-3868.
- [6] J. Heyd, G. E. Scuseria, M. Ernzerhof, *J. Chem. Phys.* **2003**, *118*, 8207–8215.